Long-range piezo-stepper actuators: Nanoscale accuracy through commutation-angle iterative learning control

LONG-RANGE PIEZO-STEPPER ACTUATORS: TOWARDS NANOSCALE ACCURACY THROUGH COMMUTATION-ANGLE ITERATIVE LEARNING CONTROL

Leontine Aarnoudse[1], Nard Strijbosch[1], Edwin Verschueren[2], and Tom Oomen[1]
[1]Control Systems Technology, Eindhoven University of Technology, Eindhoven, The Netherlands
[2] Thermo Fisher Scientific, Eindhoven, The Netherlands

BACKGROUND

Piezo-stepper actuators have major benefits in nano-positioning applications, including scanning-probe microscopy [1]. The actuators, illustrated in Figure 1, retain the high precision and high stiffness properties of the piezo elements, while achieving an infinite stroke of the mover through a walking motion. Periodic waveforms are used to map a commutation angle α to the input voltages of the piezo elements.

Engagement and release between the piezo-elements and the mover during the walking motion lead to disturbances [2]. These disturbances are directly related to the actuating waveforms, and are repeating in the commutation-angle or α-domain. Consequently, for varying velocities, the error profile caused by these disturbances is varying in the temporal domain.

Iterative Learning Control (ILC) can compensate repeating disturbances completely by modifying a feedforward signal based on preceding experiments [3]. The disturbances for a piezo-stepper actuator are repeating in the temporal domain for a constant velocity, but for varying velocities the disturbances are varying. The aim of this paper is to develop and implement an ILC approach that is applicable to long-range piezo-stepper actuators with varying velocities, by exploiting the observation that the disturbance is repeating in the α-domain.

This paper is organized as follows. First, the commutation-angle based control of a piezo-stepper actuator is explained. Then, the disturbances caused by the walking motion are analyzed. A commutation-angle iterative learning control approach is proposed to compensate these disturbances. After that, the implementation of this approach is explained and the approach is experimentally validated. In the final section, conclusions are given.

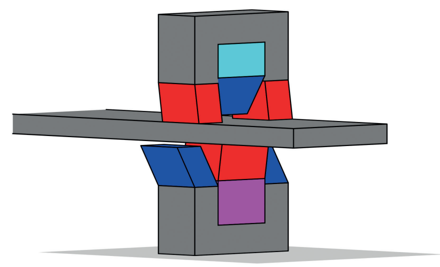

FIGURE 1. Schematic representation of a piezo-stepper actuator with clamp elements 1 (—) and 2 (—) and shear groups 1 (—) and 2 (—) indicated.

COMMUTATION-ANGLE CONTROL

In this section, the functioning and control of a piezo-stepper actuator are explained and the actuator is modeled.

The piezo-stepper actuator considered in this work consists of two groups of longitudinal and shear piezo elements, as shown in Figure 2b. When the longitudinal element or clamp of one group is elongated, the corresponding shear elements are in contact with the mover. The mover follows the position of the connected shear elements. A walking motion is obtained by alternating the connected piezo group.

The walking motion of the piezo-stepper actuator is implemented using waveforms that map a commutation angle $\alpha \in [0, 2\pi)$ [rad] to the input voltages of the piezo elements, as shown in Figure 2a. The waveforms can be divided into four phases: takeover phases 1 and 3 and reset phases 2 and 4, as shown in Figure 2.

1. Takeover phase: the clamp of group 1 is extending while that of group 2 is retracting, such that the mover is taken over by group 1. Both sets of shear elements are moving with equal velocity.

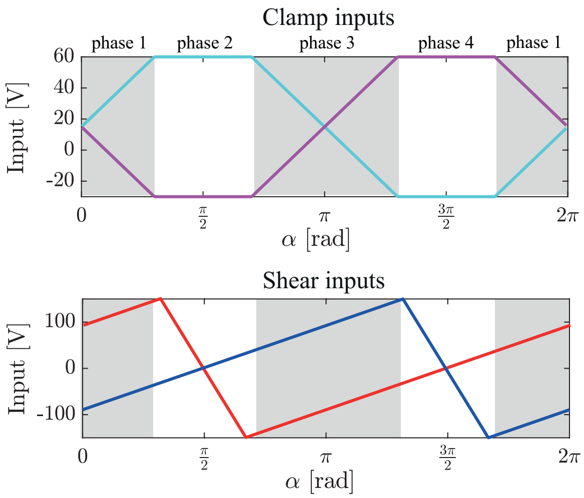

(a) Piezo-stepper actuator waveforms.

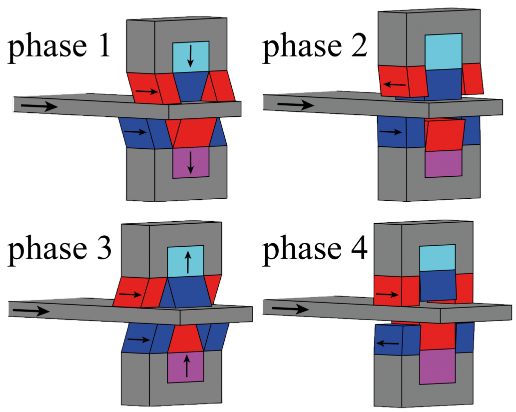

(b) Phases in a step of a piezo-stepper actuator.

FIGURE 2. The waveforms (a) map the commutation angle α to the input for the piezo elements: clamp elements 1 (—) and 2 (—) and shear groups 1 (—) and 2 (—). A step of a piezo-stepper actuator is divided into four phases, indicated in (a) and illustrated in (b). Note that in takeover phases 1 and 3, both groups may be in contact with the mover. In these phases the inputs of the shear groups have equal derivatives, such that the elements move with equal velocity.

2. Reset phase: once the clamp of group 2 is fully retracted, the shear elements of this group are reset. The shear elements of group 1 continue displacing the mover.
3. Takeover phase: the clamp of group 1 is retracting while that of group 2 is extending, such that the mover is taken over by group 2. Both sets of shear elements are moving with equal velocity.
4. Reset phase: once the clamp of group 1 is fully retracted, the shear elements of this group are reset. The shear elements of group 2 continue displacing the mover.

The piezo-stepper actuator is modeled in the α-domain as a gain with a lumped disturbance $d_\alpha(\alpha)$ [m]. The disturbance $d_\alpha(\alpha)$ is assumed to be related to the commutation angle and is analyzed in the next section. The position of the mover y [m] during a single step is described by

$$y(\alpha) = c u_s(\alpha) + d_\alpha(\alpha), \quad \alpha \in [0, 2\pi), \tag{1}$$

where c [m V^{-1}] is a positive piezo constant and u_s [V] is a combination of the inputs to the shear elements. The inputs to the two groups of shear elements are denoted by u_{s1} [V] and u_{s2} [V]. Because the derivatives of the connected shear elements are always equal, as shown in Figure 2a, the input that influences the mover can be written as a single signal $u_s(\alpha)$ for modeling. For $u_s(\alpha)$, the following holds:

$$\frac{\delta u_s(\alpha)}{\delta \alpha} = \begin{cases} \frac{\delta u_{s1}(\alpha)}{\delta \alpha} & \text{in phase 2} \\ \frac{\delta u_{s2}(\alpha)}{\delta \alpha} & \text{in phase 4} \\ \frac{\delta u_{s1}(\alpha)}{\delta \alpha} = \frac{\delta u_{s2}(\alpha)}{\delta \alpha} & \text{otherwise.} \end{cases} \tag{2}$$

Note that in this model, rate-dependent effects such as creep and hysteresis are assumed to be negligible, since these effects can be compensated, for example, by using separate feedforward [4, ch. 2,11].

The commutation angle $\alpha(t)$ is a function of time and depends on the drive frequency $f_\alpha(t)$ [Hz]. The number of steps per second is equal to the drive frequency. For each step of duration T [s], the commutation angle increases from $\alpha(0) = 0$ to $\alpha(T) = 2\pi$. The commutation angle is given by

$$\alpha(t) = 2\pi \int_0^t f_\alpha(\tau)\,\mathrm{d}\tau. \tag{3}$$

The system is modeled in terms of α for a single step. During this step, the sign of $f_\alpha(t)$ is constant and $\alpha(t) \in [0, 2\pi)$ is monotonically increasing, i.e., there is no change in direction. The time-dependency of α is omitted for brevity.

DISTURBANCE ANALYSIS

In this section, the disturbances for a piezo-stepper actuator are analyzed in the temporal and the commutation-angle domain.

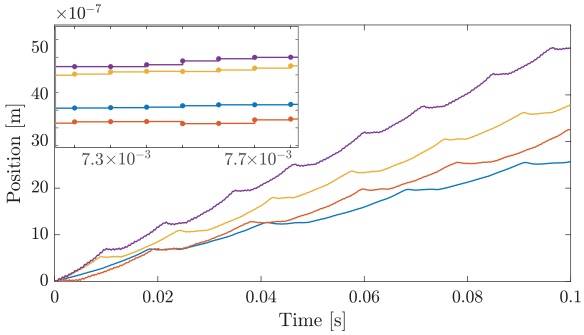

(a) Position as a function of time.

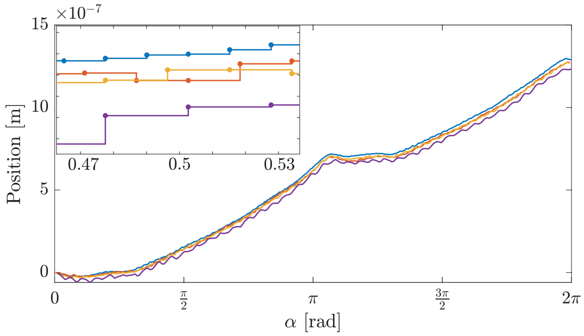

(b) Position as a function of the commutation angle.

FIGURE 3. Positions for a piezo-stepper for drive frequencies 20 Hz *(—),* 25 Hz *(—),* 30 Hz *(—) and* 40 Hz *(—). In the temporal domain (a) the sampling is equidistant but the disturbance is varying. In the α-domain (b) the sampling is non-equidistant for varying velocities, but the disturbances are similar.*

During walking experiments, disturbances in the position of the piezo-stepper actuator are observed. The desired behavior for the actuator is that for a constant drive frequency, the mover velocity is also constant. However, due to disturbances this desired behavior is not obtained, as is shown for multiple drive frequencies in Figure 3a.

Although the disturbances are varying in the temporal domain for varying drive frequencies, they are largely repeating in the commutation-angle or α-domain. This is shown in Figure 3b, where the position of the mover during a single step is plotted as a function of α for varying drive frequencies. The disturbances could be explained by considering physical sources: misalignment between the piezo elements and the mover or contact dynamics.

The central idea is to exploit the repetitiveness in the α-domain to compensate the position disturbances for the piezo-stepper actuator. To this end, an approach for commutation-angle or α-domain ILC is developed that is used to design a disturbance-compensating input as an addition to the existing waveforms.

COMMUTATION-ANGLE ITERATIVE LEARNING CONTROL

In this section, a new framework for α-domain iterative learning control is introduced. ILC can exactly compensate repeating disturbances by learning a compensating input over a series of experiments, known as iterations, while it typically amplifies non-repeating disturbances [3]. Typically, ILC is applied to systems with repetitive behavior in the temporal domain. To compensate the repeating disturbances for a piezo-stepper actuator, an α-domain approach is proposed, where each step is considered to be one iteration.

For varying drive frequencies, the number of samples per step in the α-domain is varying and samples are non-equidistant, as shown in Figure 3b. Since the sampling is iteration-varying, ILC cannot be applied directly to the sampled signals. This is resolved by parameterizing the sampled input and error signals using basis functions. ILC is then applied to the resulting continuous signals.

ILC is applied to a system that is continuous in α, given by

$$y_j(\alpha) = c(u_s(\alpha) + u_j(\alpha)) + d_\alpha(\alpha) \tag{4}$$
$$e_j(\alpha) = y_d(\alpha) - y_j(\alpha), \tag{5}$$

with disturbance-compensating input $u_j(\alpha)$, error $e_j(\alpha)$ and reference $y_d(\alpha)$ for iteration j. The error and input are parameterized such that

$$u_j(\alpha) = \psi^\top(\alpha)\theta_j^u \tag{6}$$
$$e_j(\alpha) = \psi^\top(\alpha)\theta_j^e, \tag{7}$$

where it is assumed that the basis functions can be scaled to describe the error exactly. The basis function vector ψ, containing M basis functions, and the parameter vector θ_j^u are given by

$$\psi(\alpha) = \begin{bmatrix} \psi_1(\alpha) & \psi_2(\alpha) & \dots & \psi_M(\alpha) \end{bmatrix}^\top \tag{8}$$
$$\theta_j^u = \begin{bmatrix} \theta_{1,j}^u & \theta_{2,j}^u & \dots & \theta_{M,j}^u \end{bmatrix}^\top. \tag{9}$$

The steps to implement α-domain ILC are outlined in Algorithm 1 for n iterations and explained below.

Algorithm 1 Approach to α-domain ILC

Choose a basis ψ (see next section)
for $j = 1 : n$
1: Perform an experiment of one step using u_j
2: Compute θ_j^e by determining the least squares optimal fit of the sampled error
3: Update the input parameters θ_{j+1}^u according to (10)
4: Update the input: $u_{j+1} = \psi^\top \theta_{j+1}^u$
5: Divide u_{j+1} into waveforms for the shear elements
end

Each iteration consists of five steps. First, an experiment consisting of one step of the piezo-stepper actuator is performed, resulting in an output and error according to (4) and (5). The error is parameterized according to (7), using a least squares optimal fit to find the parameter vector θ_j^e. The parameter vector for the input of the next iteration θ_{j+1}^u depends only on the previous error and input parameter vectors and is given by

$$\theta_{j+1}^u = Q_\psi \theta_j^u + L_\psi \theta_j^e, \tag{10}$$

where Q_ψ and L_ψ are optimal learning matrices. The input signal for the next iteration is determined according to (6). Extended derivations for Q_ψ and L_ψ are available as [5]. The implementation of the input signal is explained in the next section.

IMPLEMENTATION

In this section, the selection of suitable basis functions and the implementation of the input signals using waveform enhancement are explained.

The first step mentioned in Algorithm 1 is the selection of a basis ψ. This basis should be selected such that it can describe the measured error well. In this case, a set of 30 linearly independent inverse quadratic radial basis functions is used, see [6, ch.5]. The functions are of the form

$$\psi_k(\alpha) = \frac{1}{1 + (\|\alpha - c_k\|)^2}, \; k = 1, 2, ..., 30 \tag{11}$$

where the centerpoints c_k are divided equidistantly over the domain $[0, 2\pi)$. An example of a fit of an error signal with 1000 samples using this set of basis functions is shown in Figure 4.

Using the update law of (10) results in a continuous input signal $u_j(\alpha)$ for each iteration j.

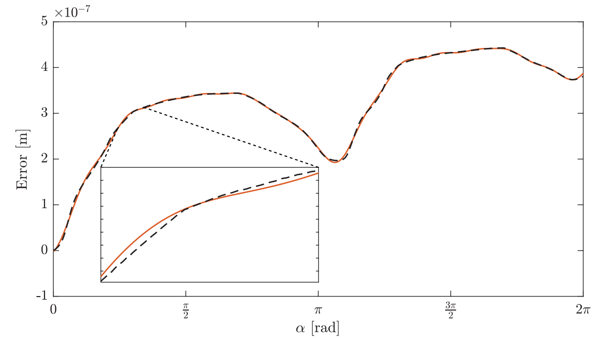

FIGURE 4. Fit (—) of the sampled error at 1000 points (- -) using 30 inverse quadratic radial basis functions.

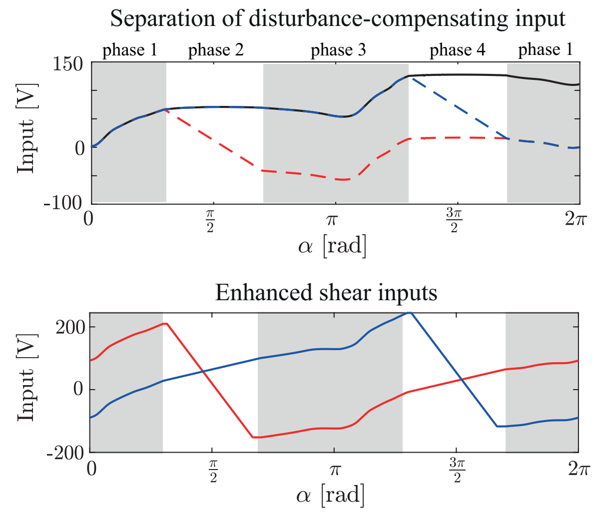

FIGURE 5. Waveform enhancement for disturbance compensation. The disturbance compensating input $u_j(\alpha)$ (—) is divided into waveforms for shear groups 1 (- -) and 2 (- -), such that the waveforms for both shear groups have equal derivatives in phases 1 and 3, where both groups may be in contact with the mover. The compensating waveforms are added to the existing shear inputs of Figure 2a, resulting in enhanced waveforms for shear group 1 (—) and 2 (—).

This single input signal cannot be implemented directly, since the input to the actuator consists of two separate shear input signals. Therefore, the disturbance-compensating input $u_j(\alpha)$ is separated into two shear input signals, such that (2) is satisfied. These signals are then added to the existing shear inputs. This procedure is illustrated in Figure 5.

EXPERIMENTAL RESULTS

The developed ILC framework is applied to a piezo-stepper actuator walking at varying

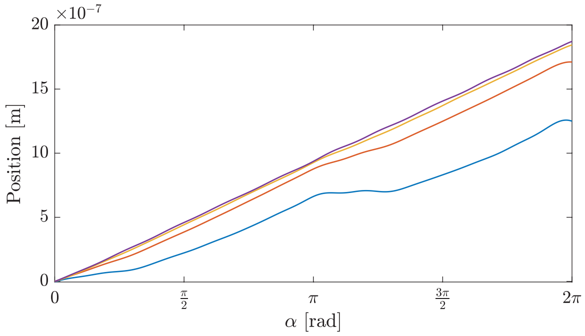

FIGURE 6. Improvements in the position of the piezo-stepper actuator for one step between iterations 1 (—), 4 (—), 8 (—) and 16 (—) using the proposed α-domain ILC framework.

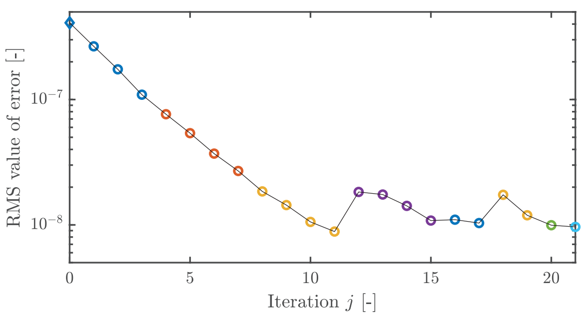

FIGURE 7. The RMS value of the error converges over iterations with iteration-varying drive frequencies: 30 Hz*(○),* 35 Hz*(○),* 25 Hz*(○),* 28 Hz*(○),* 22 Hz*(○) and* 20 Hz*(○).*

velocities for experimental validation. The desired mover position is given by the reference $y_d(\alpha) = 3 \times 10^{-7}\alpha$. The iteration-varying drive frequencies range from 20 to 35 Hz.

During the experiments, the influence of the repeating part of the disturbance is reduced significantly over iterations, as shown in Figure 6. In Figure 7 it is shown that the RMS value of the error converges to a bounded region over iterations.

Note that part of the error reduction as shown in Figure 6 and 7 is caused by convergence of the slope of the mover position to that of the reference signal. The improvements with regard to the repeating disturbance are also shown in Figure 8, where the detrended error signal before and after learning a disturbance-compensating input are compared. The experiments show that learning a disturbance-compensating signal using α-domain ILC leads to significant improvements in the positioning accuracy and jogging smoothness of the actuator.

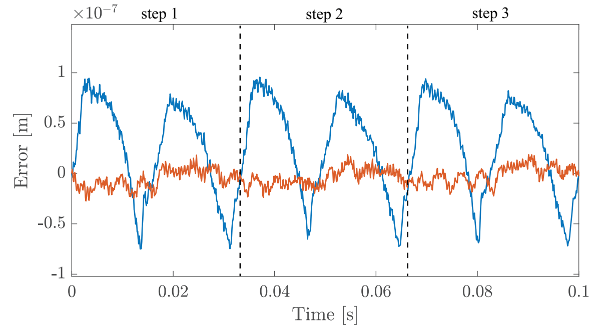

FIGURE 8. Comparsion between the detrended error for three steps at 30 Hz *before (—) and after (—) learning a disturbance compensating input.*

CONCLUSION

A new approach for iterative learning control in the commutation-angle domain is developed that can fully compensate the repeating disturbance for a piezo-stepper actuator. The approach is used to learn a disturbance-compensating input over iterations, which improves the positioning accuracy and jogging smoothness significantly. Experimental results show that the error is reduced significantly after several iterations.

REFERENCES

[1] Den Heijer M, Fokkema V, Saedi A, Schakel P, Rost MJ. Improving the accuracy of walking piezo motors. Rev Sci Instrum. 2014;85(5).

[2] Strijbosch N, Tacx P, Verschueren E, Oomen T. Commutation angle iterative learning control: Enhancing piezo-stepper actuator Waveforms. In: 8th IFAC Symp. Mechatron. Syst. Vienna, Austria; 2019. p. 1451–1456.

[3] Bristow DA, Tharayil M, Alleyne AG. A survey of iterative learning control. IEEE Control Syst. 2006;26(3):96–114.

[4] Fleming AJ, Leang KK. Design, Modeling and Control of Nanopositioning Systems. Springer; 2014.

[5] Aarnoudse L, Strijbosch N, Verschueren E, Oomen T. Commutation-Angle Iterative Learning Control for Intermittent Data: Enhancing Piezo-Stepper Actuator Waveforms. In: IFAC 21st World Congr. Berlin, Germany; 2020. .

[6] Schaback R, Wendland H. Kernel techniques: From machine learning to meshless methods. Acta Numer. 2006;15(2006):543–639.